JOURNAL OF THERMOPHYSICS AND HEAT TRANSFER
Vol. 23, No. 3, July–September 2009

Three-Dimensional Stagnation Flow and Heat Transfer on a Flat Plate with Transpiration

Ali Shokrgozar Abbassi* and Asghar Baradaran Rahimi†
Ferdowsi University of Mashhad, 91775-1111 Mashhad, Iran

DOI: 10.2514/1.41529

The existing solutions of Navier–Stokes and energy equations in the literature regarding the three-dimensional problem of stagnation-point flow, either on a flat plate or on a cylinder with or without transpiration, are only for the case of axisymmetric formulation. In this study, the nonaxisymmetric three-dimensional steady viscous stagnation-point flow and heat transfer in the vicinity of a flat plate are investigated when suction and blowing are also considered in the model. An external fluid, along z direction, with strain rate a impinges on this flat plate and produces a two-dimensional flow with different components of velocity on the plate. This external flow, as an example, can be generated in the form of multiple jet streams in a row in which the jets are in equal distances from each other along the x axis. A similarity solution of the Navier–Stokes equations and energy equation is presented in this problem. A reduction of these equations is obtained by use of appropriate similarity transformations. Velocity profiles and surface stress tensors and temperature profiles along with pressure profiles are presented for different values of velocity ratios and Prandtl number for sample cases of transpiration.

Nomenclature

a	=	constant
F, G	=	inner-region functions
f, g	=	similarity functions
Pr	=	Prandtl number
p	=	pressure
S	=	nondimensional transpiration
T	=	temperature
U, V, W	=	inviscid flow components
u, v, w	=	velocity components
W_0	=	rate of suction or blowing
x, y, z	=	Cartesian coordinates
α	=	thermal diffusivity
$\bar{\alpha}, \bar{\beta}, \bar{\gamma}, \gamma, \bar{\nu}$	=	constants
δ	=	boundary-layer thickness
ε	=	perturbation parameter
η	=	similarity variable
θ	=	nondimensional temperature
λ	=	velocity ratio in x and y directions
μ	=	viscosity
ν	=	kinetic viscosity
ξ	=	inner variable
ρ	=	density
τ	=	shear stress
Φ	=	inner-region variable

I. Introduction

THERE are many exact solutions for Navier–Stokes and energy equations regarding the problem of stagnation-point flow and heat transfer in the vicinity of a flat plate or a cylinder. Removing the nonlinearity in these problems is usually accomplished by superposition of fundamental exact solutions that lead to nonlinear coupled ordinary differential equations by separation of coordinate variables, but in all the three-dimensional cases, only axisymmetric formulation of the problem has been considered. Fundamental studies in which flows are readily superposed and/or the axisymmetric case were considered include the following papers presented in the literature: uniform shear flow over a flat plate in which the flow is induced by a plate oscillating in its own plane beneath a quiescent fluid [1]; two-dimensional stagnation-point flow [2]; the flow induced by a disk rotating in its own plane [3]; flow over a flat plate with uniform normal suction [4]; three-dimensional stagnation-point flow [5]; and axisymmetric stagnation flow on a circular cylinder [6]. Further exact solutions to the Navier–Stokes equations are obtained by superposition of the uniform shear flow and/or stagnation flow on a body oscillating or rotating in its own plane, with or without suction. The examples are as follows: superposition of two-dimensional and three-dimensional stagnation-point flows [7]; superposition of uniform suction at the boundary of a rotating disk [8]; also the solution for a fluid oscillating about a nonzero mean flow parallel to a flat plate with uniform suction given [9]; superposition of stagnation-point flow on a flat plate oscillating in its own plate, and also consideration of the case where the plate is stationary and the stagnation stream is made to oscillate [10]; uniform shear flow aligned with outflowing two-dimensional stagnation-point flow [11]; uniform flow along a flat plate with time-dependent suction and included periodic oscillations of the external stream [12]; heat transfer in an axisymmetric stagnation flow on a cylinder [13]; unsteady laminar axisymmetric stagnation flow over a circular cylinder [14]; nonsimilar axisymmetric stagnation flow on a moving cylinder [15]; transient response behavior of an axisymmetric stagnation flow on a circular cylinder due to time-dependent free-stream velocity [16]; unsteady viscous flow in the vicinity of an axisymmetric stagnation point on a cylinder [17]; shear flow over a rotating plate [18]; radial stagnation flow on a rotating cylinder with uniform transpiration [19]; suppression of turbulence in wall-bounded flows by high-frequency spanwise oscillations [20]; axisymmetric stagnation flow toward a moving plate [21]; axisymmetric stagnation-point flow impinging on a transversely oscillating plate with suction [22]; axisymmetric stagnation-point flow and heat transfer of a viscous fluid on a moving cylinder with time-dependent axial velocity and uniform transpiration [23]; axisymmetric stagnation-point flow and heat transfer of a viscous fluid on a rotating cylinder with time-dependent angular velocity and uniform transpiration [24]; and similarity solution of nonaxisymmetric heat transfer in stagnation-point flow on a cylinder with simultaneous axial and rotational movements [25]. The only three-dimensional nonaxisymmetric solution in aforementioned studies is the one in [7],

Received 10 October 2008; revision received 4 April 2009; accepted for publication 16 April 2009. Copyright © 2009 by the American Institute of Aeronautics and Astronautics, Inc. All rights reserved. Copies of this paper may be made for personal or internal use, on condition that the copier pay the $10.00 per-copy fee to the Copyright Clearance Center, Inc., 222 Rosewood Drive, Danvers, MA 01923; include the code 0887-8722/09 and $10.00 in correspondence with the CCC.

*Graduate Student.
†Professor, Faculty of Engineering; rahimiab@yahoo.com (Corresponding Author).

which is with large deviations from the correct solution because of the approximation methods used, where, in a later work [26], these deviations have been discussed.

In this study, the nonaxisymmetric three-dimensional steady viscous stagnation-point flow and heat transfer in the vicinity of a flat plate are investigated in the presence of suction and blowing by solving Navier–Stokes equations. The importance of this research work is encountered in solutions where the flow pattern on the plate is bounded in one of the directions, for example, x axis, because of whatever physical limitations. The external fluid, along z direction, with strain rate a impinges on this flat plate and produces a two-dimensional flow with different components of velocity on the plate. This external flow, as an example, can be generated in the form of multiple jet streams in a row, in which the jets are equal distances from each other along the x axis and interact with each other on the plate. A similarity solution of the Navier–Stokes equations and energy equation is derived in this problem. A reduction of these equations is obtained by use of these appropriate similarity transformations. The obtained coupled ordinary differential equations are solved using numerical techniques. Velocity profiles and surface stress tensors along with temperature profiles are presented for different values of impinging fluid strain rate, different forms of jet arrangements, Prandtl number, and sample values of suction and blowing parameters.

II. Problem Formulation

Flow is considered in Cartesian coordinates (x, y, z) with corresponding velocity components (u, v, w), see Figs. 1 and 2. In Fig. 2, a general three-dimensional stream surface along with its boundary-layer thickness is shown, which is produced because of an stagnation-point flow impinging on a flat plate where the flow pattern in x direction is bounded because of whatever physical limitation. This limitation can be generated, for example, in the form of multiple jet streams in a row in which the jets are in equal distances from each other only along the x axis and there is no limitation along the y axis. Obviously, the boundary-layer thicknesses are different in x and y directions, contrary to the case of axisymmetric flow when they are the same. Figure 2 depicts the same situation but for a certain rates of suction and blowing and their comparison with the case of no transpiration. We consider the laminar steady incompressible flow and heat transfer of a viscous fluid in the neighborhood of stagnation point on a flat plate located in the plane $z = 0$. An external fluid, along z direction, with strain rate a impinges on this flat plate and produces a two-dimensional flow with different components of velocity on the plate. This external flow, as an example, can be generated in the form of multiple jet streams in a row in which the jets are in equal distances from each other along the x axis. The steady Navier–Stokes and energy equations in Cartesian coordinates governing the flow and heat transfer are given as

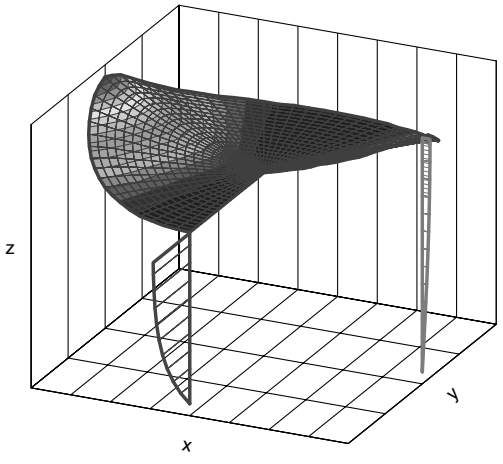

Fig. 1 Three-dimensional stream surface and velocity profiles.

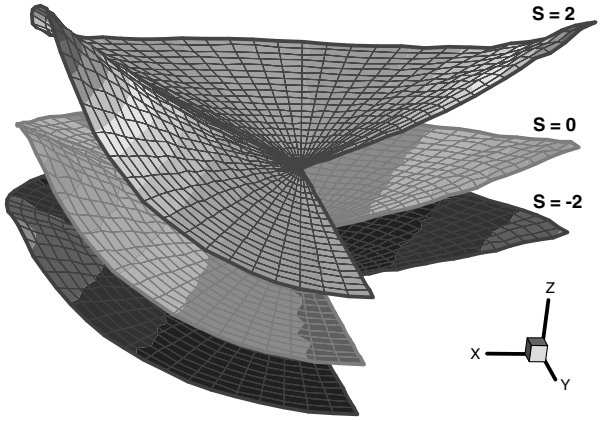

Fig. 2 Stream surface for selected values of transpiration.

Mass

$$\frac{\partial u}{\partial x} + \frac{\partial v}{\partial y} + \frac{\partial w}{\partial z} = 0 \tag{1}$$

Momentum

$$u\frac{\partial u}{\partial x} + v\frac{\partial u}{\partial y} + w\frac{\partial u}{\partial z} = -\frac{1}{\rho}\frac{\partial p}{\partial x} + \nu\left[\frac{\partial^2 u}{\partial x^2} + \frac{\partial^2 u}{\partial y^2} + \frac{\partial^2 u}{\partial z^2}\right] \tag{2}$$

$$u\frac{\partial v}{\partial x} + v\frac{\partial v}{\partial y} + w\frac{\partial v}{\partial z} = -\frac{1}{\rho}\frac{\partial p}{\partial y} + \nu\left[\frac{\partial^2 v}{\partial x^2} + \frac{\partial^2 v}{\partial y^2} + \frac{\partial^2 v}{\partial z^2}\right] \tag{3}$$

$$u\frac{\partial w}{\partial x} + v\frac{\partial w}{\partial y} + w\frac{\partial w}{\partial z} = -\frac{1}{\rho}\frac{\partial p}{\partial z} + \nu\left[\frac{\partial^2 w}{\partial x^2} + \frac{\partial^2 w}{\partial y^2} + \frac{\partial^2 w}{\partial z^2}\right] \tag{4}$$

Energy

$$u\frac{\partial T}{\partial x} + v\frac{\partial T}{\partial y} + w\frac{\partial T}{\partial z} = \alpha\left[\frac{\partial^2 T}{\partial x^2} + \frac{\partial^2 T}{\partial y^2} + \frac{\partial^2 T}{\partial z^2}\right] \tag{5}$$

where p, ρ, ν, and α are the fluid pressure, density, kinematic viscosity, and thermal diffusivity, respectively.

III. Self-Similar Solution

A. Fluid Flow Solution

The classical potential flow solution of the governing Eqs. (1–4) is as follows, in which we have exerted the parameter λ in x direction component of velocity to introduce three-dimensionality:

$$U = a\lambda x, \qquad 0 < \lambda \leq 1 \tag{6}$$

$$V = ay \tag{7}$$

$$W = -a(\lambda + 1)z - W_0 \tag{8}$$

$$P_\infty = P_0 - \tfrac{1}{2}\rho a^2[\lambda^2 x^2 + y^2 + (\lambda + 1)^2 z^2 + W_0^2 - 2aW_0(\lambda + 1)z] \tag{9}$$

where p_0 is stagnation pressure and λ is the coefficient which indicates the difference between the velocity components in x and y directions. The velocity components in these directions are the same if $\lambda = 1$, indicating that each of the two adjacent single jets are far enough from each other and therefore there are no interactions between them. W_0 is the suction or blowing rate in z direction.

A reduction of the Navier–Stokes equations is sought by the following coordinate separation, in which the solution of the viscous problem inside the boundary layer is obtained by composing the

inviscid and viscous parts of the velocity components as the following:

$$u = a\lambda x f'(\eta), \qquad 0 < \lambda \leq 1 \tag{10}$$

$$v = ay[f'(\eta) + g'(\eta)] \tag{11}$$

$$w = -\sqrt{a\nu}[g(\eta) + (\lambda + 1)f(\eta)] - W_0 \tag{12}$$

$$\eta = \sqrt{a/\nu}z \tag{13}$$

in which the terms involving $f(\eta)$ and $g(\eta)$ in Eqs. (10–12) comprise the Cartesian similarity form for steady stagnation-point flow and the prime denotes differentiation with respect to η. Note, boundary layer is defined here as the edge of the points where their velocity is 99% of their corresponding potential velocity. Transformation Eqs. (10–13) satisfy Eq. (1) automatically and their insertion into Eqs. (2–4) yields a coupled system of ordinary differential equations in terms of $f(\eta)$ and $g(\eta)$ and an expression for the pressure

$$f''' + [(\lambda + 1)f + g - S]f'' + \lambda[1 - (f')^2] = 0 \tag{14}$$

$$g''' + [(\lambda + 1)f + g - S]g'' - [g' + 2f']g' - (1 - \lambda)[(f')^2 - 1] = 0 \tag{15}$$

$$\begin{aligned} p(x, y, z) = P_0 - \frac{\rho a^2}{2}[\lambda^2 x^2 + y^2] + \tfrac{1}{2}\rho a^3 S[S\nu - 2\sqrt{a\nu}(\lambda + 1)z] \\ - \rho a\nu\{\tfrac{1}{2}[(\lambda + 1)f + g]^2 + (f' + g') + \lambda f' - (\lambda + 1)] \\ + \rho a\nu[\eta(\lambda + 1)(\gamma - aS)\} \end{aligned} \tag{16}$$

Relation (16), which represents pressure, is obtained by integrating Eq. (4) in z direction and by use of the potential flow solution Eqs. (6–9) as boundary conditions. The function $g(\eta)$ outside the boundary-layer region is independent of the variable η and equal to a constant value γ. Therefore,

$$\gamma = \lim_{\eta \to \infty} g(\eta) = \text{Const.}$$

and

$$S = \frac{W_0}{\sqrt{a\nu}} \qquad S > 0 \text{ (suction)} \qquad S < 0 \text{ (blowing)}$$

The boundary conditions for the coupled differential Eqs. (14) and (15) are

$$\eta = 0\text{: } f = 0, \qquad f' = 0, \qquad g = 0, \qquad g' = 0 \tag{17}$$

$$\eta \to \infty\text{: } f' = 1, \qquad g' = 0 \tag{18}$$

Note that, when $\lambda = 1$, the case of axisymmetric three-dimensional results are obtained (Homman [5]). When $\lambda = 0$, the results are the same as the two-dimensional problem.

B. Heat Transfer Solution

To transform the energy equation into a nondimensional form for the case of defined wall temperature, we introduce

$$\theta = \frac{T(\eta) - T_\infty}{T_w - T_\infty} \tag{19}$$

Making use of transformation Eqs. (10–13), the energy equation may be written as

$$\theta'' + Pr \times \theta'[g + (\lambda + 1)f - S] = 0 \tag{20}$$

with the boundary conditions as

$$\eta = 0 \qquad \theta = 1 \tag{21}$$

$$\eta \to \infty \qquad \theta = 0 \tag{22}$$

where $Pr = \nu/\alpha$ is the Prandtl number and the prime indicates differentiation with respect to η.

Note that, for $Pr = 1$, the thickness of the fluid boundary layer and heat boundary layer become the same, and therefore this concept is proved by reaching Eq. (20) from Eq. (14) through substitution of $\theta = f'$.

Equations (14), (15), and (20) are solved numerically using a shooting method trial and error and based on the Runge–Kutta algorithm, and the results are presented for selected values of λ and Pr in following sections. Because Eqs. (14) and (15) are coupled, we guess a value for $g(\eta)$ function first and solve Eq. (14) for $f(\eta)$. Then Eq. (15) is integrated and a new value of $g(\eta)$ is obtained, which is used to solve Eq. (14) again. This procedure is repeated until the difference of the results is less than 0.00001.

IV. Shear Stress

The shear stress at the wall surface is calculated from

$$\tau = \mu\left(\frac{\partial u}{\partial z}\mathbf{e}_x + \frac{\partial v}{\partial z}\mathbf{e}_y\right)_{z=0} \tag{23}$$

where μ is the fluid viscosity. Using the transformation Eqs. (10–13), the shear stress at the flat plate surface becomes

$$\tau = \rho\nu^{\frac{1}{2}}a^{\frac{3}{2}}[\lambda^2 x^2 f''^2 + y^2(f'' + g'')^2]^{\frac{1}{2}} \tag{24}$$

This quantity is presented for different values of λ in later sections.

V. Asymptotic Analysis

Asymptotic results for large values of Prandtl numbers are given in this section. Assuming

$$\varepsilon = 1/Pr \tag{25}$$

as a perturbation parameter, energy Eq. (20) can be written as

$$\varepsilon\theta'' + [g + (1 + \lambda)f - S]\theta' = 0 \tag{26}$$

Since ε appears in front of the highest-order term, an inner and outer analysis is needed to obtain a composite solution for all the values of Prandtl numbers. A perturbation expansion in outer region is assumed as

$$\theta(\eta, \varepsilon) = \theta_0(\eta) + \varepsilon\theta_1(\eta) + \mathcal{O}(\varepsilon^2) \tag{27}$$

Substitution of this expansion into Eq. (26) and collecting the coefficients of the powers of ε and setting them equal to zero gives typical equations as

$$\theta_0'(\eta) = 0 \tag{28}$$

which solves to $\theta_0(\eta) = \text{constant}$. Therefore, the outer solution is introduced as $\theta^0(\eta) = \text{constant}$.

To obtain the inner solution, we consider the following stretching of the variables:

$$\begin{aligned} \xi = \eta/\varepsilon^{\bar{\nu}}, \qquad F(\xi) = f(\eta)/\varepsilon^{\bar{\alpha}} \\ G(\xi) = g(\eta)/\varepsilon^{\bar{\beta}}, \qquad \Phi(\xi) = \theta(\eta)/\varepsilon^{\bar{\gamma}} \end{aligned} \tag{29}$$

Substitution of these new variables into Eqs. (14), (15), and (26) and taking the distinguished limits (Nayfeh [27]) would result in

$$\bar{\nu} = 3/5, \qquad \bar{\alpha} = \bar{\beta} = 2/5, \qquad \bar{\gamma} = 0 \tag{30}$$

Therefore, the energy equation governing the inner region (inside the boundary layer) would be

$$\Phi'' + [G + (\lambda + 1)F - S]\Phi' = 0 \tag{31}$$

in which the prime indicates differentiation with respect to ξ. Intersection of the solutions of this equation with the outer solution

would bring about uniformly valid solutions throughout the region for all values of Prandtl numbers.

VI. Presentation of Results

In this section, the solution of the self-similar Eqs. (14), (15), and (20) along with the surface shear stresses for different values of velocity ratios and Prandtl numbers are presented.

The boundary-layer thickness in the two directions on the flat plate versus the velocity ratio is presented in Fig. 3 for selected values of suction and blowing. This thickness is larger in x direction compared to y direction because of the difference of the velocity components in these directions, and the difference of the boundary-layer thickness in these directions decreases as λ increases until the value of unity where these two layers meet each other, which is a validation of our results compared to the axisymmetric problem case. From this figure, the following relations can be obtained for the boundary-layer thickness versus the ratio of the velocities in potential flow:

For $S = 0$,

$$\delta_x = -0.75\lambda + 2.75 \qquad \delta_y = -0.35\lambda + 2.35$$

For $S = 2$,

$$\delta_x = -0.1\lambda^{2.7} - 0.014\lambda + 2.99 \qquad \delta_y = -0.1\lambda^{1.95} + 2.96$$

And for $S = -2$,

$$\delta_x = 0.1\lambda^{2.1} - 0.45\lambda + 1.61 \qquad \delta_y = -0.15\lambda^{1.2} - 0.01\lambda + 1.49$$

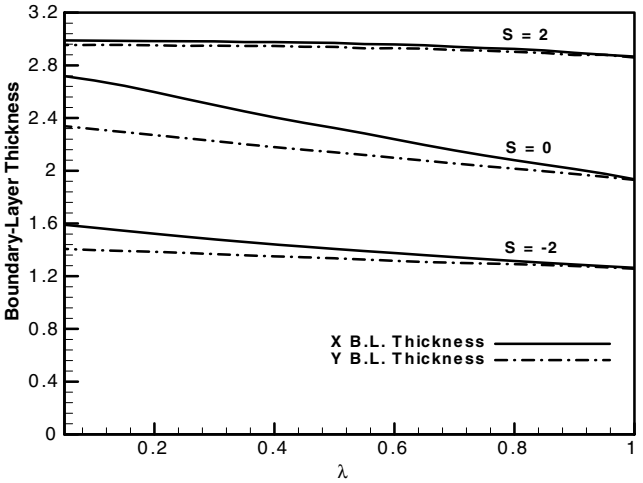

Fig. 3 Boundary-layer thickness versus variation of velocity ratio and selected values of suction and blowing.

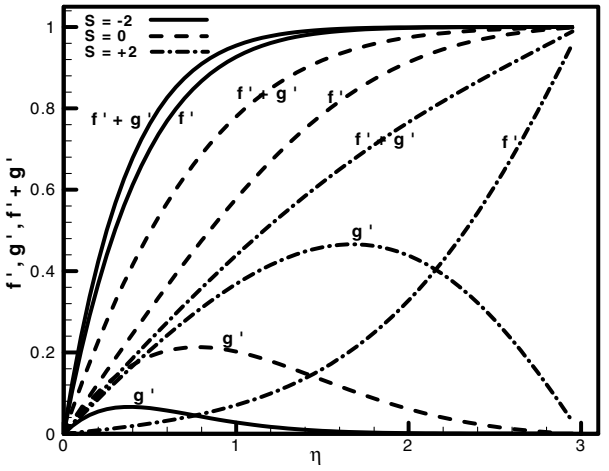

Fig. 4 Typical u and v velocity components for $\lambda = 0.05$ and selected values of suction and blowing.

Figures 4–7 present the profiles of f', g', and $f' + g'$ for different values of velocity ratio λ and selected values of transpirations. The smaller the λ, the bigger g', and therefore the difference between the velocity components is larger. For $\lambda \to 1$, then $g' \to 0$, and the two velocity components become the same, which is again a validation of our result compared to the axisymmetric problem case.

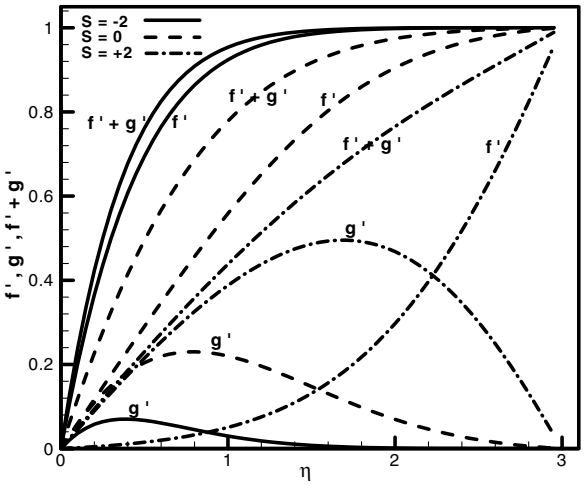

Fig. 5 Typical u and v velocity components for $\lambda = 0.1$ and selected values of suction and blowing.

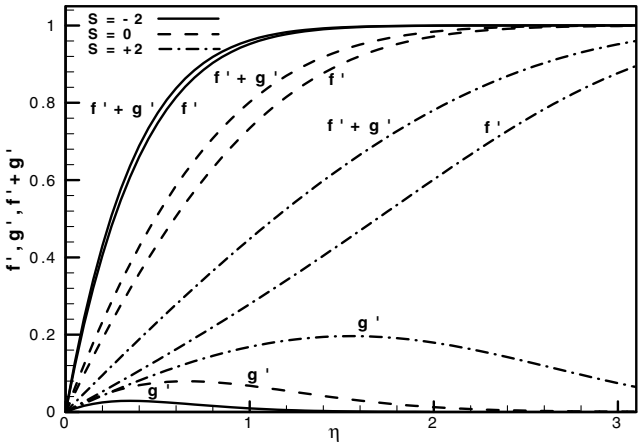

Fig. 6 Typical u and v velocity components for $\lambda = 0.5$ and selected values of suction and blowing.

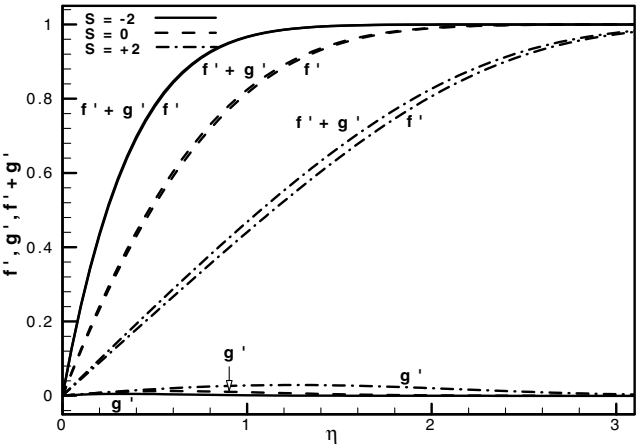

Fig. 7 Typical u and v velocity components for $\lambda = 0.9$ and selected values of suction and blowing.

Figures 8–11 depict the f and g profiles, and therefore the w component of velocity for different values of velocity ratio and for selected values of suction and blowing. The bigger the λ, the larger the absolute value of the w component of the velocity, as expected. This component of velocity, which is the penetration of momentum into the boundary layer in the z direction, changes abruptly as λ increases because the boundary layer increases faster as this parameter gets larger, and therefore there is need for more penetration of the momentum and hence this component of velocity gets bigger. The effect of blowing is in the direction of increasing the w component of velocity and suction in the direction of decreasing it, as expected. It is interesting to note that, as $\lambda \to 0$ (for example, $\lambda = 0.05$), the flow governing differential equations appears in the new form of

$$f''' + (f+g)f'' = 0$$
$$g''' + (f+g)g'' - (g' + 2f')g' + [1 - (f')^2] = 0$$

Which are definitely different with the governing equations of the two-dimensional problem case [2], because λ tends to zero gradually and the basic governing equations remain three-dimensional. Note that the existence of the physical limitation in x direction is the cause of the gradual change of λ from one to zero.

The temperature profiles for different values of velocity ratio and selected values of Prandtl numbers and transpiration are presented in Figs. 12–23. Increase of velocity ratio and increase of Prandtl number both cause the decrease of the temperature profile. It is also noted that, for $\lambda \to 1$ and $Pr = 1$, the temperature boundary layer is obtained the same as the velocity boundary layer and is also a validation of the nonaxisymmetric temperature compared to the axisymmetric problem case.

In presenting the uniform value of temperature profiles for higher Prandtl numbers ($Pr = 10.0$), an asymptotic method has been used. These uniform values of temperature profiles have been obtained from matching an outer solution with an inner solution.

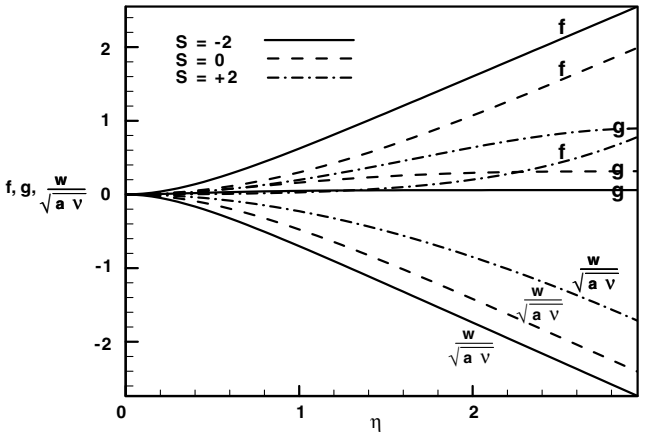

Fig. 8 Typical w component of velocity for $\lambda = 0.05$ and selected values of suction and blowing.

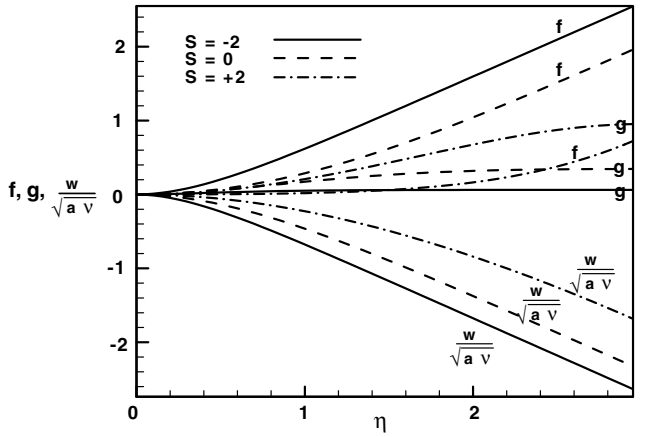

Fig. 9 Typical w component of velocity for $\lambda = 0.1$ and selected values of suction and blowing.

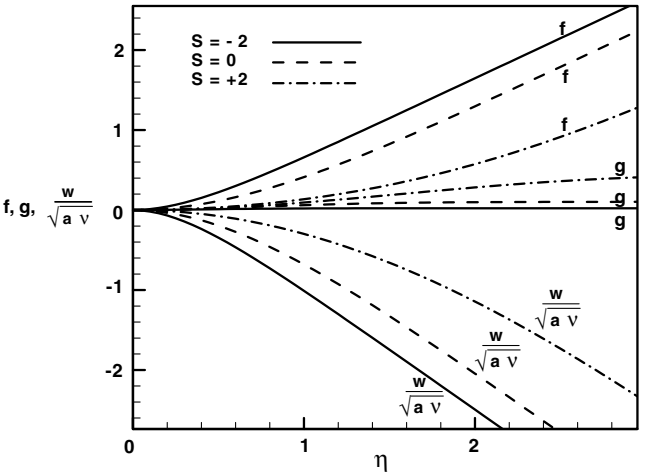

Fig. 10 Typical w component of velocity for $\lambda = 0.5$ and selected values of suction and blowing.

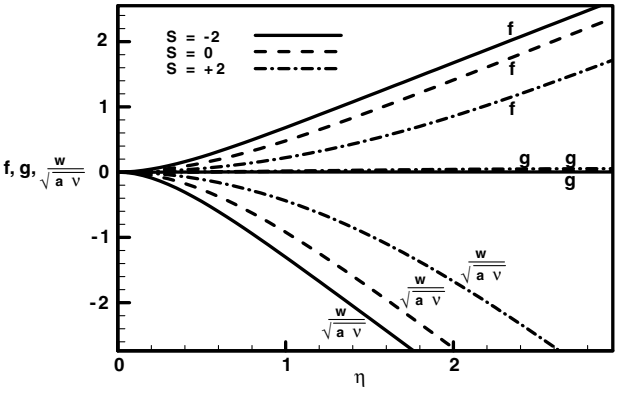

Fig. 11 Typical w component of velocity for $\lambda = 0.9$ and selected values of suction and blowing.

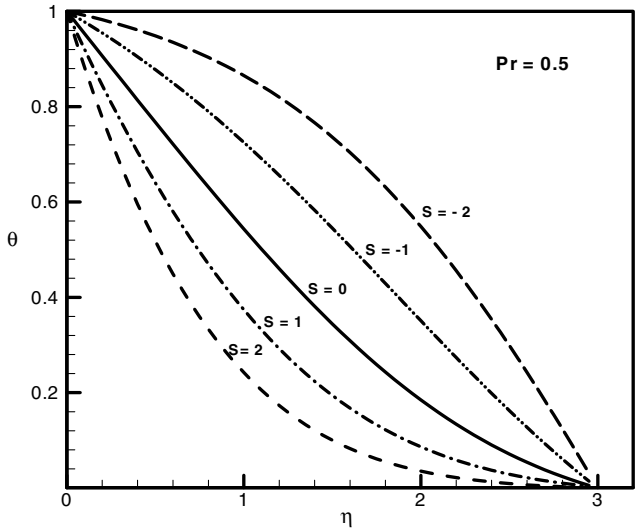

Fig. 12 Temperature profile for $\lambda = 0.01$ and $Pr = 0.5$ for selected values of suction and blowing.

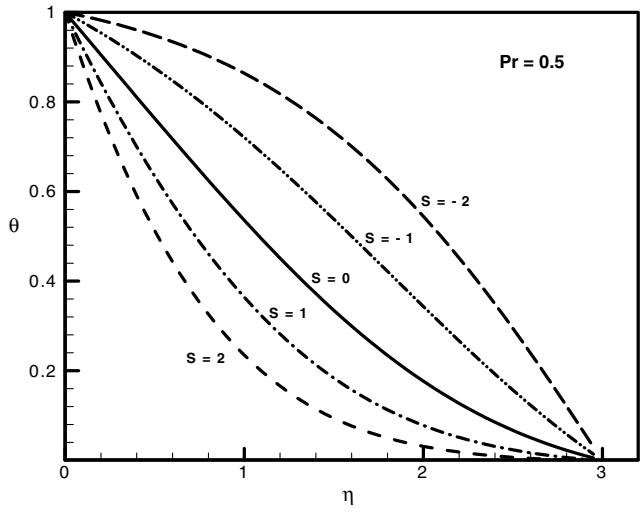

Fig. 13 Temperature profile for $\lambda = 0.1$ and $Pr = 0.5$ for selected values of suction and blowing.

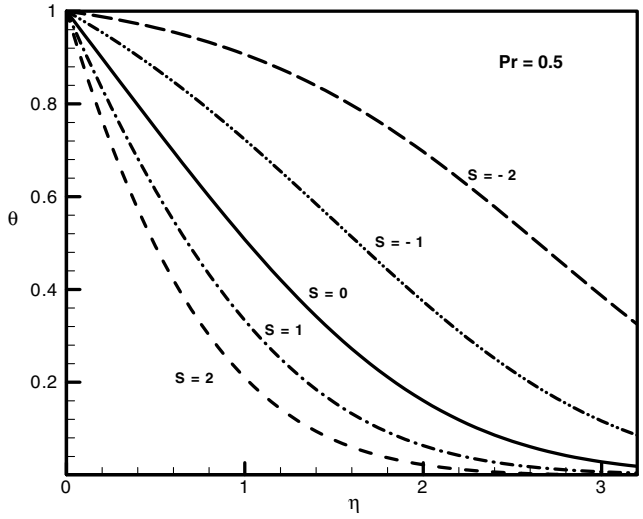

Fig. 14 Temperature profile for $\lambda = 0.5$ and $Pr = 0.5$ for selected values of suction and blowing.

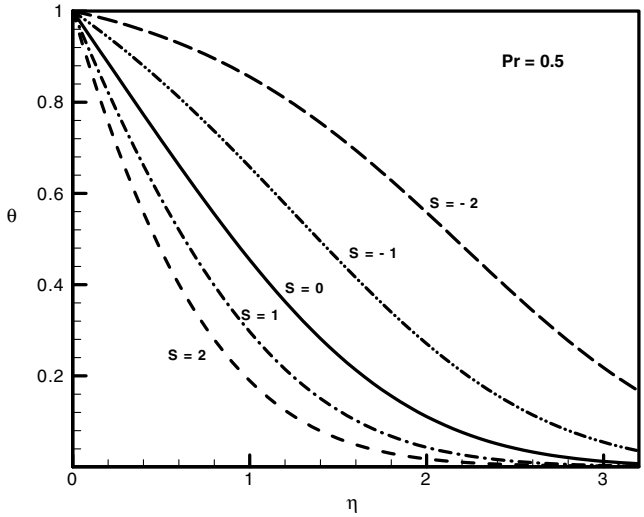

Fig. 15 Temperature profile for $\lambda = 0.9$ and $Pr = 0.5$ for selected values of suction and blowing.

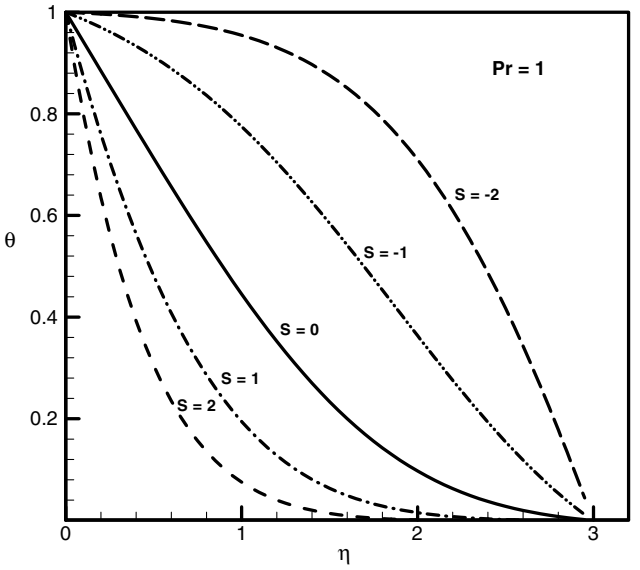

Fig. 16 Temperature profile for $\lambda = 0.01$ and $Pr = 1.0$ for selected values of suction and blowing.

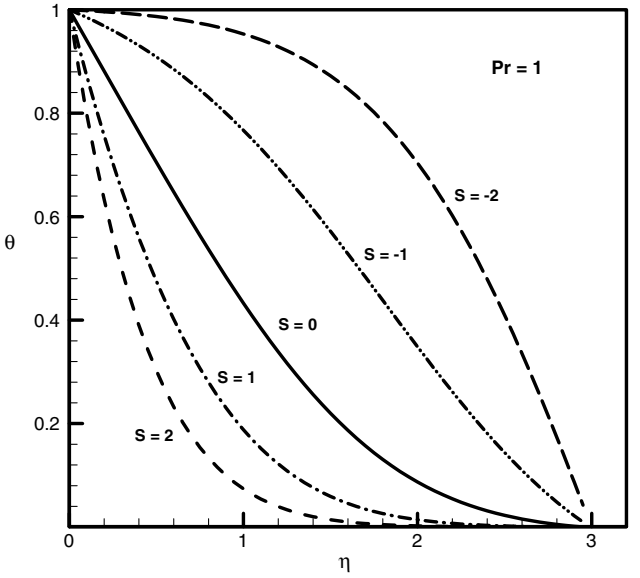

Fig. 17 Temperature profile for $\lambda = 0.1$ and $Pr = 1.0$ for selected values of suction and blowing.

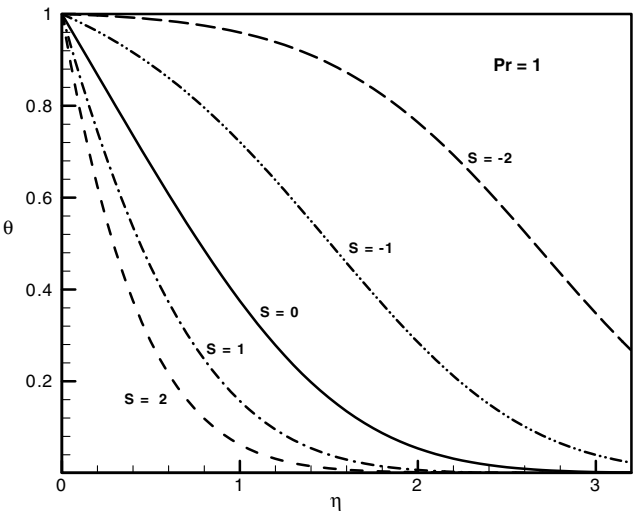

Fig. 18 Temperature profile for $\lambda = 0.5$ and $Pr = 1.0$ for selected values of suction and blowing.

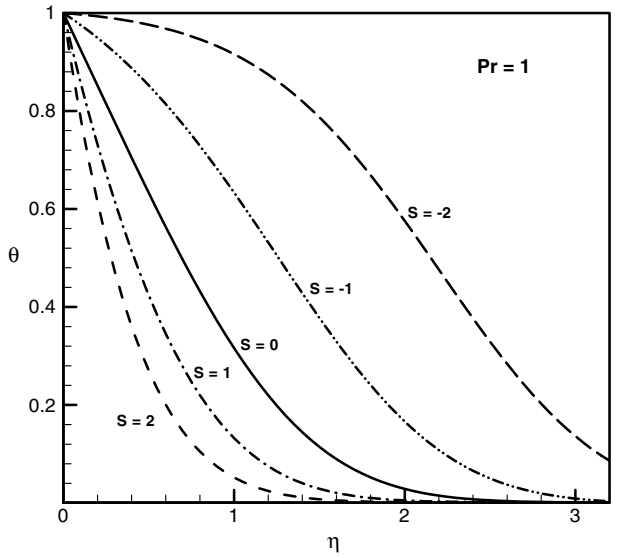

Fig. 19 Temperature profile for $\lambda = 0.9$ and $Pr = 1.0$ for selected values of suction and blowing.

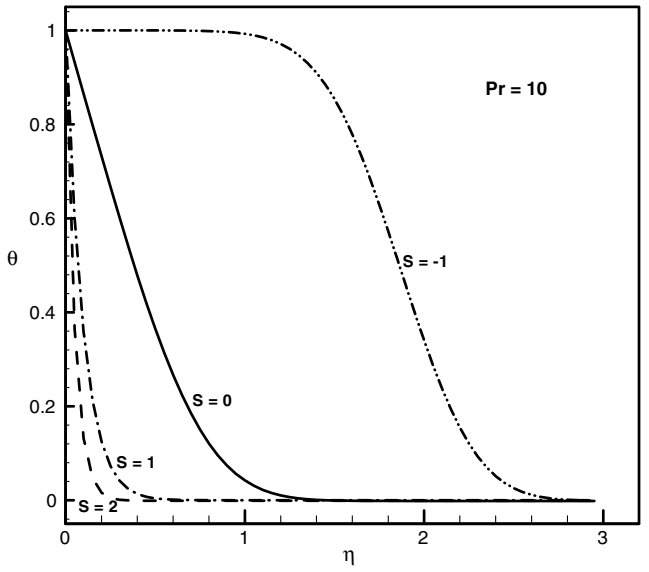

Fig. 20 Temperature profile for $\lambda = 0.01$ and $Pr = 10.0$ for selected values of suction and blowing.

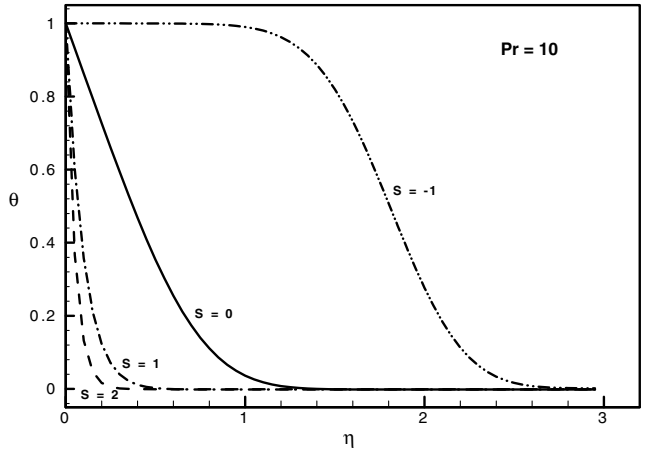

Fig. 21 Temperature profile for $\lambda = 0.1$ and $Pr = 10.0$ for selected values of suction and blowing.

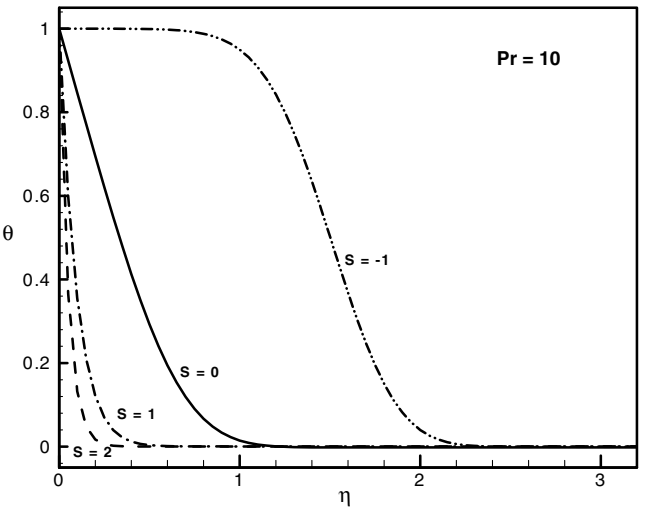

Fig. 22 Temperature profile for $\lambda = 0.5$ and $Pr = 10.0$ for selected values of suction and blowing.

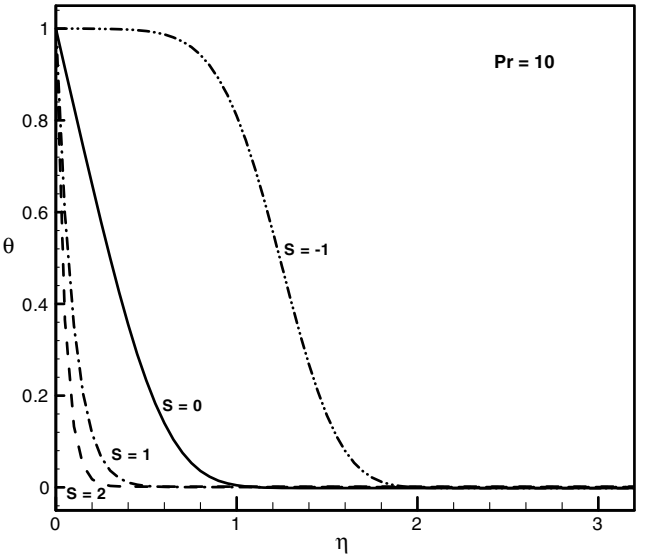

Fig. 23 Temperature profile for $\lambda = 0.9$ and $Pr = 10.0$ for selected values of suction and blowing.

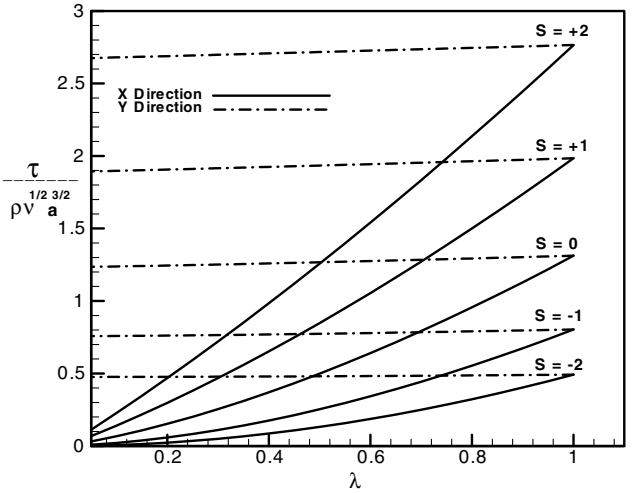

Fig. 24 Shear stress in x and y directions versus λ and selected values of suction and blowing.

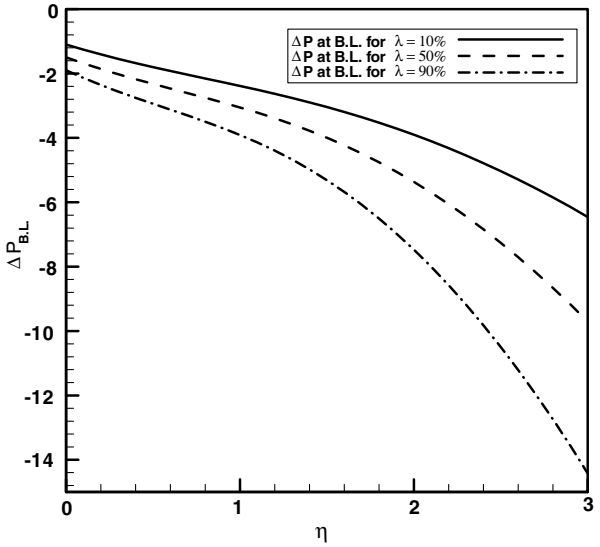

Fig. 25 Pressure profiles for selected values of λ and $S = 0$.

Figure 24 presents the change of surface shear stress on the flat plate in terms of velocity ratio λ. The following relations can be deduced from this plot:

For $S = 0$,

$$\tau_x = \lambda^{1.55} + 0.3\lambda \qquad \tau_y = 0.1\lambda^{1.1} - 0.03\lambda + 1.235$$

For $S = 2$,

$$\tau_x = 1.5\lambda^{1.32} + 1.25\lambda + 0.02 \qquad \tau_y = 0.0951\lambda + 2.67$$

For $S = -2$,:

$$\tau_x = 0.45\lambda^{2.08} + 0.05\lambda \qquad \tau_y = 0.01\lambda^{2.5} + 0.006\lambda + 0.476$$

As $\lambda \to 0$, the stress tensor in x direction tends to zero, but note that $\lambda = 0$ does not represent a physical situation.

Pressure profiles inside the boundary layer are shown in Fig. 25 for selected values of λ. From these profiles, it can be seen that, with increase of velocity ratio in x and y directions and tending toward the symmetric situation, variation of pressure inside the boundary layer increases, because λ affects velocity directly and pressure changes with velocity in power form.

VII. Conclusions

The effects of suction and blowing have been presented in this problem using a similarity solution of the Navier–Stokes equations and energy equation for nonaxisymmetric three-dimensional stagnation-point flow and heat transfer on a flat plate. This task has been accomplished by choosing appropriate similarity transformations and reduction of these governing equations to a system of coupled ordinary differential equations and subsequent numerical integration. Velocity components, temperature profiles, pressure change, surface stress tensor, and asymptotic solution of temperature profile for a high Prandtl case have been presented for selected values of velocity ratios. Increase of velocity and thermal boundary-layer thicknesses are encountered in all cases for blowing and their decrease in the case of suction. These differences have been compared with the case of no transpiration for selected values of these parameters. This problem represents many physical situations including the stagnation-point problem, in which the impinging flow is generated in the form of multiple jet streams in a row where the jets are equal distances from each other along one axis.

References

[1] Stokes, G. G., "On the Effect of the Internal Friction of Fluids on the Motion of Pendulum," *Transactions of the Cambridge Philosophical Society*, Vol. 9, Pt. 2, 1851, pp. 8–106.

[2] Hiemenz, K., "Boundary Layer for a Homogeneous Flow Around a Dropping Cylinder," *Dinglers Polytechnic Journal*, Vol. 326, 1911, pp. 321–324.

[3] Von Kármán, T., "About Laminar and Turbulence Friction," *Zeitschrift fuer Angewandte Mathematik und Mechanik*, Vol. 1, 1921, pp. 233–252.

[4] Griffith, A. A., and Meredith, F. W., "The Possible Improvement in Aircraft Performance Due to the Use of Boundary Layer Suction," Royal Aircraft Establishment Rept. No. E 3501, p. 12.

[5] Homman, F. Z., "Der EINFLUSS GROSSER Zahighkeit bei der Strmung um den Zylinder und um die Kugel," *Zeitschrift fuer Angewandte Mathematik und Mechanik*, Vol. 16, No. 3, 1936, pp. 153–164.
doi:10.1002/zamm.19360160304

[6] Wang, C. Y., "Axisymmetric Stagnation Flow on a Cylinder," *Quarterly of Applied Mathematics*, Vol. 32, 1974, pp. 207–213.

[7] Howarth, L., "The Boundary Layer in Three-Dimensional Flow, Part II: The Flow Near Stagnation Point," *Philosophical Magazine*, Ser. 7, Vol. 42, 1951, pp. 1433–1440.

[8] Stuart, J. T., "On the Effects of Uniform Suction on the Steady Flow Due to a Rotating Disk," *Quarterly Journal of Mechanics and Applied Mathematics*, Vol. 7, No. 4, 1954, pp. 446–457.
doi:10.1093/qjmam/7.4.446

[9] Stuart, J. T., "A Solution of the Navier–Stokes and Energy Equations Illustrating the Response of Skin Friction and Temperature of an Infinite Plate Thermometer to Fluctuations in the Stream Velocity," *Proceedings of the Royal Society of London A*, Vol. 231, No. 1184, 1955, pp. 116–130.
doi:10.1098/rspa.1955.0160

[10] Glauert, M. B., "The Laminar Boundary Layer on Oscillating Plates and Cylinders," *Journal of Fluid Mechanics*, Vol. 1, No. 1, 1956, pp. 97–110.
doi:10.1017/S002211205600007X

[11] Stuart, J. T., "The Viscous Flow Near a Stagnation-Point when the External Flow has Uniform Vorticity," *Journal of Aerospace Science and Technology*, Vol. 26, 1959, pp. 124–125.

[12] Kelly, R. E., "The Flow of a Viscous Fluid past a Wall of Infinite Extent with Time-Dependent Suction," *Quarterly Journal of Mechanics and Applied Mathematics*, Vol. 18, No. 3, 1965, pp. 287–298.
doi:10.1093/qjmam/18.3.287

[13] Gorla, R. S. R., "Heat Transfer in an Axisymmetric Stagnation Flow on a Cylinder," *Applied Scientific Research*, Vol. 32, No. 5, 1976, pp. 541–553.
doi:10.1007/BF00385923

[14] Gorla, R. S. R., "Unsteady Laminar Axisymmetric Stagnation Flow over a Circular Cylinder," *Development in Mechanics*, Vol. 9, 1977, pp. 286–288.

[15] Gorla, R. S. R., "Nonsimilar Axisymmetric Stagnation Flow on a Moving Cylinder," *International Journal of Engineering Science*, Vol. 16, No. 6, 1978, pp. 397–400.
doi:10.1016/0020-7225(78)90029-0

[16] Gorla, R. S. R., "Transient Response Behavior of an Axisymmetric Stagnation Flow on a Circular Cylinder Due to Time-Dependent Free Stream Velocity," *Letters in Applied and Engineering Sciences*, Vol. 16, No. 7, 1978, pp. 493–502.

[17] Gorla, R. S. R., "Unsteady Viscous Flow in the Vicinity of an Axisymmetric Stagnation-Point on a Cylinder," *International Journal of Engineering Science*, Vol. 17, No. 1, 1979, pp. 87–93.
doi:10.1016/0020-7225(79)90009-0

[18] Wang, C. Y., "Shear Flow over a Rotating Plate," *Applied Scientific Research*, Vol. 46, No. 1, 1989, pp. 89–96.
doi:10.1007/BF00420004

[19] Cunning, G. M., Davis, A. M. J., and Weidman, P. D., "Radial Stagnation Flow on a Rotating Cylinder with Uniform Transpiration," *Journal of Engineering Mathematics*, Vol. 33, No. 2, 1998, pp. 113–128.
doi:10.1023/A:1004243728777

[20] Jung, W. L., Mangiavacchi, N., and Akhavan, R., "Suppression of Turbulence in Wall-Bounded Flows by High-Frequency Spanwise Oscillations," *Physics of Fluids*, Vol. A4, Aug. 1992, pp. 1605–1607.

[21] Wang, C. Y., "Axisymmetric Stagnation Flow Towards a Moving Plate," *AIChE Journal*, Vol. 19, No. 5, Sept. 1973, pp. 1080–1081.
doi:10.1002/aic.690190540

[22] Weidman, P. D., and Mahalingam, S., "Axisymmetric Stagnation-Point Flow Impinging on a Transversely Oscillating Plate with Suction," *Journal of Engineering Mathematics*, Vol. 31, No. 4, 1997, pp. 305–318.
doi:10.1023/A:1004211515780

[23] Saleh, R., and Rahimi, A. B., "Axisymmetric Stagnation-Point Flow

and Heat Transfer of a Viscous Fluid on a Moving Cylinder with Time-Dependent Axial Velocity and Uniform Transpiration," *Journal of Fluids Engineering*, Vol. 126, No. 6, 2004, pp. 997–1005. doi:10.1115/1.1845556

[24] Rahimi, A. B., and Saleh, R., "Axisymmetric Stagnation-Point Flow and Heat Transfer of a Viscous Fluid on a Rotating Cylinder with Time-Dependent Angular Velocity and Uniform Transpiration," *Journal of Fluids Engineering*, Vol. 129, Jan. 2007, pp. 106–115. doi:10.1115/1.2375132

[25] Rahimi, A. B., and Saleh, R., "Similarity Solution of Unaxisymmetric Heat Transfer in Stagnation-Point Flow on a Cylinder with Simultaneous Axial and Rotational Movements," *Journal of Heat Transfer*, Vol. 130, No. 5, 2008, pp. 054502.1–054502.5. doi:10.1115/1.2885173

[26] Shokrgozar, A. A., and Rahimi, A. B., "Non-Axisymmetric Three-Dimensional Stagnation-Point Flow and Heat Transfer on a Flat Plate," *Journal of Fluids Engineering*, Vol. 131, No. 7, 2009, pp. 074501.1–074501.5. doi:10.1115/1.3153366

[27] Nayfeh, A. H., *Perturbation Techniques*, Wiley, New York, 1985.